Theory for detection of 2D and 1D plasmon dispersion relations by ricochet electron energy loss spectra

1989 J. Phys.: Condens. Matter 1 8453

(http://iopscience.iop.org/0953-8984/1/44/016)

J. Phys.: Condens. Matter 1 (1989) 8453–8469. Printed in the UK

Theory for detection of 2D and 1D plasmon dispersion relations by ricochet electron energy loss spectra

P Longe† and S M Bose‡

†Institut de Physique, B5, Université de Liège, Sart-Tilman, B-4000 Liège, Belgium

‡Department of Physics and Atmospheric Science, Drexel University, Philadelphia, PA 19104, USA

Received 6 December 1988

Abstract. When a beam of electrons is incident quasiparallel on the surface of a metal, on a two-dimensional electron gas, or on the axis of a one-dimensional electron gas, these electrons have a high probability of undergoing a ricochet scattering with excitation of a plasmon. The scattering cross section peaks along critical directions of emergence, which depend on the energy ε_k of the scattered electrons. Experimental determination of these directions as a function of ε_k can yield direct information on the plasmon dispersion relation. Numerical calculations are presented for ricochet scattering on the surface of aluminum, an accumulation layer on ZnO and a one-dimensional conductor.

1. Introduction

In a recent theoretical paper (Longe and Bose 1986) we proposed a photoemission experiment which could yield the values of the parameters ($\omega_s(0)$, μ_D and n) of the surface plasmon dispersion relation $\omega_s(q) = \omega_s(0) + \mu_D q^n$ of a metal. We have shown that the photoelectrons emitted along the metal surface from atoms located at a small distance outside the surface have a high probability to ricochet with the excitation of a surface plasmon if the angle of emergence α is less than a critical angle $\alpha_M(\varepsilon_k)$, where $\varepsilon_k = k^2/2m$ is the energy of the outgoing electron. Moreover, the lineshape $I(\varepsilon_k, \alpha)$ of the surface plasmon satellite has a peak at $\alpha = \alpha_M(\varepsilon_K)$. By locating this peak one determines the function $\alpha_M(\varepsilon_k)$ which yields direct information on the form and parameters of the above dispersion rule. The proposed experiment, however, presents two difficulties. First, the production rate of the photoelectrons is weak in the direction of the metal surface when emitted so close to the surface, and second, the spectral resolution of the photoelectrons is determined by the linewidth of the ionised core level.

In this paper, we propose yet another experiment in which these difficulties can be avoided. In this experiment, the photoelectrons are replaced by an external beam of monoenergetic electrons which are allowed to be scattered by a sample placed with its surface quasiparallel to the beam. We have calculated the scattering cross section for ricochet energy losses by surface plasmon production and have shown that such a relatively more flexible experiment could yield the same information on the dispersion relations of a wider variety of two-dimensional plasmons (Ritchie 1963, Ritchie and Marusak 1966, Stern 1967, Ando *et al* 1982, Fetter 1973, Vinter 1975, Allen *et al* 1977,

0953-8984/89/448453 + 17 $02.50

Goldstein *et al* 1980, Many *et al* 1981, Giuliani and Quinn 1984, Grimes 1978†). This type of experiment can even be extended to one-dimensional plasmons, such as those propagating in chains of molecules.

In these experiments, the only input data are the energy $\varepsilon_p = p^2/2m$ of the incoming electron beam and the small angle θ it makes with the surface of the sample (two-dimensional (2D) electron gas), or the axis of the chain (one-dimensional (1D) electron gas). In this latter case the experiment can be performed using a system of parallel chains of molecules situated in a plane, the projection of momentum $\boldsymbol{p}$ on the plane being parallel to the axis of the chains. The chains will be assumed to be sufficiently segregated as to produce only a weak overlap between the electron wavefunctions of the different chains.

In other words only two components $\boldsymbol{p}_\perp$ and $\boldsymbol{p}_\parallel$ of $\boldsymbol{p}$ (parallel and perpendicular to the sample surface, respectively) are given and chosen such that $p_\perp/p \simeq \theta \ll 1$. One measures the angular distribution of the scattered electrons, i.e. the differential cross section $\sigma(\varepsilon_k, \alpha, \beta)$ where $\varepsilon_k = k^2/2m$ is the outgoing energy, and α and β are two small angles giving the direction of the outgoing beam (vector $\boldsymbol{k}$). Copolar angle α is measured in the plane $(\boldsymbol{p}, \boldsymbol{p}_\perp)$ perpendicular to the sample surface and azimuthal angle β is measured along this surface. The scattering first satisfies the energy conservation

$$p^2 = k^2 + 2m\omega_D(q) \tag{1}$$

where $\omega_D(q)$ is the energy or frequency ($\hbar = 1$) of a D-dimensional plasmon of momentum $\boldsymbol{q}$. We must also have momentum conservation

$$\boldsymbol{p}_\parallel = \boldsymbol{k}_\parallel + \boldsymbol{q}. \tag{2}$$

This vector equation has the dimension D of $\boldsymbol{q}$ (or of the plasmon). These two conditions prescribe geometric conditions to the experiments such that the relevant parameters are defined in rather narrow ranges. Condition (1) describes the conservation of energy before and after the interaction of the electron with the plasmon field, a condition which does not have to be strictly satisfied as long as the duration of this interaction is short. This is the case in the usual EELS experiments where the 2D-plasmon energy losses can indeed be observed simply because of the quantum character of the process. What we propose here is an experiment where the geometric situation is such that condition (1) is strictly satisfied, together with (2), as it should be in a classical system. In such a case, we will see that the differential cross section $\sigma(\varepsilon_k, \alpha, \beta)$ presents a sharp peak when the values of angles θ, α and β are small. The detection of this peak as a function of α, or of β, and of the outgoing energy ε_k could yield direct information on the parameters defining the plasmon dispersion relation, e.g. $\omega_D(q) = \omega_D(0) + \mu_D q^n$. It is the relation between the intensity and the position of the peak of $\sigma(\varepsilon_k, \alpha, \beta)$ and the parameters of the dispersion relation (here $\omega_D(0)$, μ_D and n) that we intend to discuss in the present paper.

In § 2 we present a calculation of the cross section which is valid for any dimensionality of the plasmon. Such a general presentation is interesting for it emphasises the relation between the scattering potential of the plasmon field acting on an external electron, and the dynamic properties of the plasmon inside a D-dimensional electron gas. In § 3, we discuss the explicit form of $\sigma(\varepsilon_k, \alpha, \beta)$ and the geometric requirements prescribed by the conservation laws (1) and (2). In § 4 we present an explicit calculation of σ for various geometries and emphasise the relation between σ and the parameters of $\omega_D(q)$.

† Grimes (1978) concerns electrons in surface states on liquid helium.

2. Plasmon scattering cross section

The differential cross section can be written in the general form

$$\sigma(\boldsymbol{k}) \equiv \sigma(\varepsilon_k, \alpha, \beta) = \Omega^{-1} \sum_{q} \delta(\varepsilon_p - \varepsilon_k - \omega_D(q)) |f_q(\hat{\boldsymbol{k}})|^2 \tag{3}$$

where Ω is the D-dimensional 'volume' occupied by the plasmon modes (i.e. the volume, area or length of the sample containing the D-dimensional electron gas) and where $f_q(\hat{\boldsymbol{k}})$ is the Born scattering amplitude which depends on direction $\hat{\boldsymbol{k}}$, the wavefunction of the scattered electron being $e^{i\boldsymbol{p}\cdot\boldsymbol{x}} + (e^{ikr}/r) f_q(\hat{\boldsymbol{k}})$. One has

$$f_q(\hat{\boldsymbol{k}}) = -\frac{m}{2\pi} \int d^3x \; e^{-i(\boldsymbol{k}-\boldsymbol{q})\cdot\boldsymbol{x}} U_q(\boldsymbol{x}). \tag{4}$$

Note that the Born approximation based on plane waves is reasonable as we are dealing with high-energy electrons. The deviation from the plane-wave behaviour due to interaction energies is minimal. In fact, our previous calculations of photoemission spectra of metals (Bose *et al* 1981, 1983), with and without the plane-wave approximation, show that the higher-energy electrons can indeed be treated as plane waves. The problem now consists of determining the scattering potential $U_q(\boldsymbol{x})$ of the plasmon field in (4). By symmetry this potential can be written as

$$U_q(\boldsymbol{x}) = e^{-i\boldsymbol{q}\cdot\boldsymbol{x}_\parallel} U(\boldsymbol{q}, \boldsymbol{x}_\perp) \Theta(\Delta x_\parallel \in \Omega). \tag{5}$$

Here and below symbols $\perp$ and $\parallel$ denote the vector components respectively perpendicular and parallel to 'volume' Ω (for the plasmon $\boldsymbol{q}_\perp = 0$, hence $\boldsymbol{q} \equiv \boldsymbol{q}_\parallel$). The step function Θ means that the position vector $\boldsymbol{x}_\parallel$ varies only inside the 'volume' Ω of the sample. Note that for a three-dimensional sample (bulk) which we will also consider for the sake of generality, one has $\boldsymbol{x}_\perp = 0$, and $\boldsymbol{x}_\parallel \equiv \boldsymbol{x}$.

From (3), (4) and (5) one obtains

$$\sigma(\boldsymbol{k}) = \Omega(m/2\pi)^2 \delta(\varepsilon_p - \varepsilon_k - \omega_D(q)) \left| \int d^{3-D}x_\perp \; e^{-i(\boldsymbol{k}_\perp - \boldsymbol{q}_\perp)\cdot\boldsymbol{x}_\perp} U(\boldsymbol{q}, \boldsymbol{x}_\perp) \right|^2 \tag{6}$$

where $\boldsymbol{q} = \boldsymbol{k}_\parallel - \boldsymbol{p}_\parallel$ is implicitly assumed.

To calculate (6) for various geometries we need an explicit form of $U(\boldsymbol{q}, \boldsymbol{x}_\perp)$ which has been derived in the appendix as

$$U(\boldsymbol{q}, \boldsymbol{x}_\perp) = v(\boldsymbol{q}, \boldsymbol{x}_\perp)[\omega_D(q)/2v_0(\boldsymbol{q})]^2 \tag{7}$$

where $v(\boldsymbol{q}, \boldsymbol{x}_\perp)$ is the Coulomb potential and where $v_0(\boldsymbol{q}) \equiv v(\boldsymbol{q}, 0)$. We will now proceed to the calculation of the differential scattering cross section for the three cases $D = 3, 2$ and 1.

2.1. *Three-dimensional gas*

The case $D = 3$ is a well known situation which we present here for the sake of completeness in our survey of the problem. The calculation is straightforward. Since $\boldsymbol{x}_\parallel \equiv \boldsymbol{x}$, $v(\boldsymbol{q}, \boldsymbol{x}_\perp)$ reduces to $v(\boldsymbol{q}) = v_0(\boldsymbol{q}) = 4\pi e^2/q^2$, and from (6) and (7) one has

$$\sigma(\varepsilon_k, \hat{\boldsymbol{k}}) = \Omega(m/2\pi)^2 [\omega_3(q) v(q)/2] \delta(\varepsilon_p - \varepsilon_k - \omega_3(q))$$

with $\boldsymbol{q} = \boldsymbol{p} - \boldsymbol{k}$. The total cross section

$$\sigma_{tot} = \int d\varepsilon_k \int d^2\hat{k} \; \sigma(\varepsilon_k, \hat{\boldsymbol{k}}) = \int d^3k \; \sigma(\boldsymbol{k})/mk$$

can be calculated immediately for a dispersionless plasmon ($\omega_3 = \omega_p$) assuming

$q < q_c \ll p$. One obtains

$$\sigma_{tot}/\Omega = 1/\lambda(\varepsilon_p) = (me^2/p)^2\omega_p \ln(pq_c/m\omega_p)$$

which is the well known electron (inverse) mean-free path for bulk plasmon excitations. In this three-dimensional situation, the external electron penetrates into the bulk electron gas and undergoes multiple scattering due to electron–hole excitations. This makes the measurement of the delicate angular dependence of $\sigma(\varepsilon_k, \hat{\boldsymbol{k}})$ practically impossible, contrary to the $D = 2$ and $D = 1$ cases, which are the main topics of this paper.

2.2. Two-dimensional gas (and also surface excitation of three-dimensional gas)

Since $D = 2$, let us write $\boldsymbol{x}_\parallel = (x, y)$, $\boldsymbol{x}_\perp = (z)$ and $\boldsymbol{q} = (q_x, q_y)$. This gives

$$v(\boldsymbol{q}, \boldsymbol{x}_\perp) \equiv v(q, z) = \frac{1}{2\pi}\int_{-\infty}^{\infty} \frac{\mathrm{d}q_z\, \mathrm{e}^{\mathrm{i}q_z z} 4\pi e^2}{(q^2 + q_z^2)}$$

$$= 2\pi e^2\, \mathrm{e}^{-q|z|}/q$$

and $v_0(q) = v(q, 0) = 2\pi e^2/q$. Hence from (7) one has

$$U(q, z) = (\omega_2(q)\pi e^2/q)^{1/2}\, \mathrm{e}^{-q|z|}$$

and from (6) we have

$$\sigma(\varepsilon_k, \hat{\boldsymbol{k}}) = A(m/2\pi)^2\delta(\varepsilon_p - \varepsilon_k - \omega_2(q))\omega_2(q)(\pi e^2/q)$$

$$\times \left| \int_{-\infty}^{\infty} \mathrm{d}z\Theta(z) \exp[-\mathrm{i}(k_z - p_z)z - q|z|] \right|^2$$

$$= A(m/2\pi)^2\delta(\varepsilon_p - \varepsilon_k - \omega_2(q))[\pi e^2\omega_2(p)/q(\boldsymbol{p} - \boldsymbol{k})^2] \tag{8}$$

with $\boldsymbol{q} = \boldsymbol{k}_\parallel - \boldsymbol{p}_\parallel$ and with A (area) standing for Ω. Note that in (8) a step function $\Theta(z)$ has been introduced to take into account the fact that the incident electron is not supposed to enter the sample. If it penetrates into the sample ($z < 0$) it will undergo multiple scatterings and will not be properly detected, a situation similar to that encountered above for the bulk case ($D = 3$).

2.3. One-dimensional case

Here we assume $\boldsymbol{x}_\parallel = (z)$, $\boldsymbol{x}_\perp = (x, y)$ and $\boldsymbol{q} = (q_z)$. This gives

$$v(\boldsymbol{q}, \boldsymbol{x}_\perp) \equiv v(q_z, \rho) = \int_{-\infty}^{\infty} \frac{\mathrm{d}z\, \mathrm{e}^{-\mathrm{i}q_z z} e^2}{(\rho^2 + z^2)^{1/2}}$$

$$= 2e^2 K_0(q\rho)$$

where $\rho = |\boldsymbol{x}_\perp|$, $q = |q_z|$ and where K_0 is the modified Bessel function of order zero. Hence one has

$$v_0(q_z) = v(q_z, 0) = 2e^2 K_0(0)$$

which diverges! To avoid this divergence one has to use the fact that ρ is not strictly zero inside the one-dimensional sample (chain) and is at least of the order of the radius of

the sample or equivalently of the order a^{-1} of the transverse part of the electron wavefunction. Since $K_0(x) \sim -\ln(xe^{\gamma}/2)$ for $x \ll 1$ (γ is the Euler constant), we can write

$$v_0(q_z) = 2e^2 \ln(a/q).$$

Therefore (7) becomes

$$U(q_z, \rho) = [e^2\omega_1(q)/\ln(a/q)]^{1/2} K_0(q\rho)$$

and from (6) one has

$$\sigma(\varepsilon_k, \hat{\boldsymbol{k}}) = L(m/2\pi)^2 \delta(\varepsilon_p - \varepsilon_k - \omega_1(q))[e^2\omega_1(q)/\ln(a/q)]$$
$$\times \left| \int \mathrm{d}^2 x_\perp K_0(q\rho) \exp[-\mathrm{i}(\boldsymbol{k}_\perp - \boldsymbol{p}_\perp) \cdot \boldsymbol{x}_\perp] \right|^2$$

with $q = |k_z - p_z|$ and L (length) standing for Ω. The integral in the above expression can be performed exactly using the identity $\int_0^\infty \mathrm{d}\rho\rho K_0(q\rho) J_0(k\rho) = 1/(q^2 + k^2)$. One obtains

$$\sigma(\varepsilon_k, \hat{\boldsymbol{k}}) = L\delta(\varepsilon_p - \varepsilon_k - \omega_1(q)) m^2 e^2 \omega_1(q)/((\boldsymbol{p} - \boldsymbol{k})^4 \ln(a/q)). \tag{9}$$

3. Angular dependence of the scattered beam

As indicated in the Introduction, the differential cross sections (8) and (9) present a peak (δ-function) when the following two conditions are satisfied:

$$p^2 - k^2 - \nu(q) = 0 \tag{10}$$

and

$$\boldsymbol{q} = \boldsymbol{p}_\parallel - \boldsymbol{k}_\parallel. \tag{11}$$

For notational simplicity we have written $\nu(q) \equiv 2m\omega_D(q)$. At this time we proceed to calculate the explicit angular dependence of the scattering cross sections for both two- and one-dimensional cases.

3.1. Two-dimensional case

In the $D = 2$ (surface plasmon) case, $\sigma(\varepsilon_k, \alpha, \beta)$ is given by (8). Once the magnitudes of $\boldsymbol{p}_\parallel, \boldsymbol{p}_\perp$ and $\boldsymbol{k}$ (or equivalently θ, ε_p and ε_k) are fixed the magnitude of $\boldsymbol{q}$ is defined by (10) and, as shown in figure 1, the vector $\boldsymbol{k}$ has to be on the intersection of a sphere of radius k and a thin circular cylinder of radius q, with its axis perpendicular to the sample surface and located at a point defined by $\boldsymbol{p}_\parallel$. Because of the ricochet condition required by the denominator of (8), $|\boldsymbol{p} - \boldsymbol{k}|$ as well as q, and hence $|\boldsymbol{p}_\perp - \boldsymbol{k}_\perp|$, are small compared to p and k. In other words, the relevant part of the intersection corresponds to only that part which belongs to small scattering angles α and β. A look at figures 1 and 2 shows that for these small scattering angles, the intersection can be approximated by an ellipse or

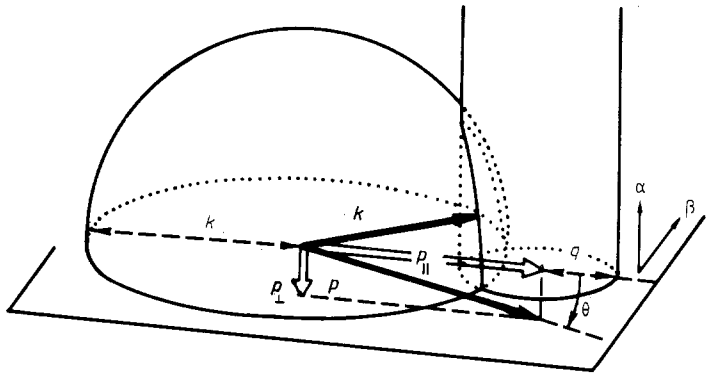

Figure 1. This figure shows the geometry that the vectors $\boldsymbol{p}$, $\boldsymbol{k}$ and $\boldsymbol{q}$ must satisfy (excitation of a two-dimensional plasmon). The head of vector $\boldsymbol{k}$ lies along the intersection of a sphere of radius k and a circular cylinder of radius q with its axis through the point $\boldsymbol{p}_{\|}$. The directions of copolar angle α and azimuthal angle β of $\boldsymbol{k}$ are pointed out. (This figure is not to scale.)

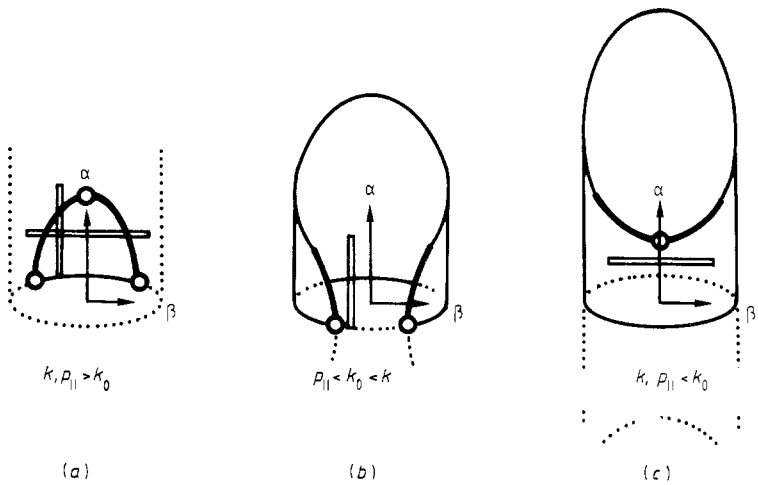

Figure 2. This figure shows three possible shapes of the intersection, mentioned in figure 1, for the various possible values of k, $p_{\|}$ and k_0. The intersection represented is found when viewed in the direction of the outgoing beam. The appropriate orientation of the detector slit to locate β_M or α_M (open circles) is also indicated. (This figure is not to scale.)

by two hyperbolae, depending on the sign of $p_{\|} - k$. In fact in the (α, β) space shown in figure 2, the intersection can be described by a quadratic expression

$$k^2 = k_0^2 + P\alpha^2 + Q\beta^2 \tag{12}$$

which must be equivalent to (10) with q given by (11), i.e. by

$$q^2 = (k_{\|} - k\cos\alpha\cos\beta)^2 + (-k\cos\alpha\sin\beta)^2$$

$$\simeq (p_{\|} - k)^2 + k(p_{\|} - k)\alpha^2 + p_{\|}k\beta^2. \tag{13}$$

Momentum k_0 in (12) and associated q_0 are obtained by solving the set of equations (10) and (13) for $\alpha = \beta = 0$, which are

$$p^2 - k_0^2 - \nu(q_0) = 0 \tag{14a}$$

$$q_0^2 = (p_\parallel - k_0)^2. \tag{14b}$$

Expression (12) is then obtained by expanding (10) for small $k^2 - k_0^2$ and using q defined by (13). One finds

$$P = (p_\parallel - k_0)/R = q_0 \operatorname{sgn}(p_\parallel - k_0)/R \tag{15a}$$

$$Q = p_\parallel/R \tag{15b}$$

with

$$R = 2q_0/(k_0\nu'(q_0)) - (p_\parallel - k_0)/k_0^2$$

$$\simeq 2q_0/(p\nu'(q_0)) \tag{16}$$

and $\nu'(q) = \mathrm{d}\,\nu(q)/\mathrm{d}q$.

From (12) and (15*a*), it is clear that the nature of the intersection depends on the relative magnitude of k_0, k and $p_\parallel$. For $k < k_0 < p_\parallel$ there is no intersection; for k and $p_\parallel > k_0$ the relevant part of the intersection is an ellipse (figure 2(*a*)); for $p_\parallel < k_0 < k$ and for k and $p_\parallel < k_0$, one has two types of hyperbolae (bold lines in figure 2(*b*, *c*)). The radius of the cylinder being much smaller than that of the sphere, the intersections are in fact much more elongated than depicted in figure 2.

By using (12) and related expansions, the differential cross section (8) can then be written in the form

$$\sigma(k, \alpha, \beta)/A = [S/D(\alpha, \beta)]\delta(k^2 - k_0^2 - P\alpha^2 - Q\beta^2) \tag{17}$$

with

$$S = m^2e^2\nu(q_0)/(4\pi p^2 q_0) \tag{18}$$

and

$$D(\alpha, \beta) = (\nu(q_0)/2p^2)^2 + (\alpha + \theta)^2 + \beta^2. \tag{19}$$

This denominator $D(\alpha, \beta)$ is small due to the ricochet conditions.

From an observational viewpoint it is interesting to determine the extremal angles $\alpha = \alpha_M$ and $\beta = \beta_M$ indicated by open circles in figure 2. To do this the outgoing beam could be picked up by a narrow slit detector placed parallel to the α (or β) axis. The slit can be moved in the β (or α) direction. In such a scanning a sharp drop in the measured intensity will occur for $\alpha = \alpha_M$ (or $\beta = \beta_M$), i.e. the extremal angular position (open circles). In the situation depicted by figure 2(*b*) the slit, represented by a double line, is parallel to the α axis and a β scanning is performed. Conversely in figure 2(*c*), the slit is parallel to the β axis to perform an α-scanning. In figure 2(*a*) (ellipse) both techniques could be used.

First let us consider the case where the slit is parallel to the α axis. The outgoing beam is collected for all values of α between 0 and $\Delta\alpha$ ($\Delta\alpha$ is the angular length of the slit). Note that the negative values of α are not detected here since they correspond to a beam having penetrated into the sample. In such a device one measures

$$A^{-1}\sigma(k,\beta) = A^{-1}\int_0^{\Delta\alpha} \mathrm{d}\alpha\ \sigma(k,\alpha,\beta) \tag{20}$$
$$= S\Theta(\mathscr{A})/(2D(\sqrt{\mathscr{A}},\beta)|P|\sqrt{\mathscr{A}})$$

with $\mathscr{A} = (k^2 - k_0^2 - Q\beta^2)/P$. As indicated before this cross section presents a sharp peak for $\mathscr{A} = 0$ above (or below) which it cancels. Equation $\mathscr{A} = 0$ is equivalent to

$$\beta_M = (k^2 - k_0^2)/Q \tag{21}$$
$$= 2q_0(k^2 - k_0^2)/(p^2\nu'(q_0)).$$

This expression of β_M as a function of the outgoing energy ε_k is important, since its experimental determination gives direct information on the plasmon dispersion relation. The first numerical application presented in § 4 is related to the detection of this β_M (surface plasmon of metals).

Next we consider the case of the detector slit parallel to the β axis and scanning the beam along the α axis. Here all values of β between $-\Delta\beta$ and $\Delta\beta$ can be collected, $\Delta\beta$ corresponding to the half-length of the slit. One measures

$$A^{-1}\sigma(k,\alpha) = A^{-1}\int_{-\Delta\beta}^{\Delta\beta} \mathrm{d}\beta\ \sigma(k,\alpha,\beta)$$
$$= S\Theta(\mathscr{B})/(D(\alpha,\sqrt{\mathscr{B}})Q\sqrt{\mathscr{B}}) \tag{22}$$

with $\mathscr{B} = (k^2 - k_0^2 - P\alpha^2)/Q$. Again this cross section presents a sharp peak for $\mathscr{B} = 0$ followed by a sudden cancellation. This structure corresponds to

$$\alpha_M = (k^2 - k_0^2)/P$$
$$= 2\,\mathrm{sgn}(p_\parallel - k_0)(k^2 - k_0^2)/(p\nu'(q_0)). \tag{23}$$

This critical angle when detected as a function of k^2 will also give information on the plasmon dispersion relation. This α scanning is particularly suitable for the two-dimensional 'acoustic' plasmon (see the second application in § 4.2 which concerns the plasmons in accumulation layers on ZnO).

3.2. One-dimensional case

This situation is in a sense simpler than the above two-dimensional case. Equation (11) is replaced by $q_z = p_z - k_z$ or

$$q = |p_z - k_z| \tag{24}$$

where p_z and k_z play the roles of the previous $\boldsymbol{p}_\parallel$ and $\boldsymbol{k}_\parallel$. Again, once the magnitudes of $p_z, p_\perp$ and k (or equivalently θ, ε_p and ε_k) are fixed, vector $\boldsymbol{k}$ can geometrically be defined to be on the intersection of two surfaces. But here the thin cylinder of figure 1 is replaced by a pair of parallel planes, perpendicular to the chain (z axis) and cutting it at points $k_z = p_z - q_z = p_z - q$ (figure 3(*a*)).

Like the two-dimensional case, we can work in an (α, β) space. Angles α and β locate the direction of $\boldsymbol{k}$ from the z axis. These angles are measured in two perpendicular planes passing by the z axis, the α plane containing vector $\boldsymbol{p}$. The second plane (β plane) may have a physical meaning. If we consider a *system* of parallel molecular chains, it will be the plane containing the chains, or a surface plane if these chains are embedded in a bulk

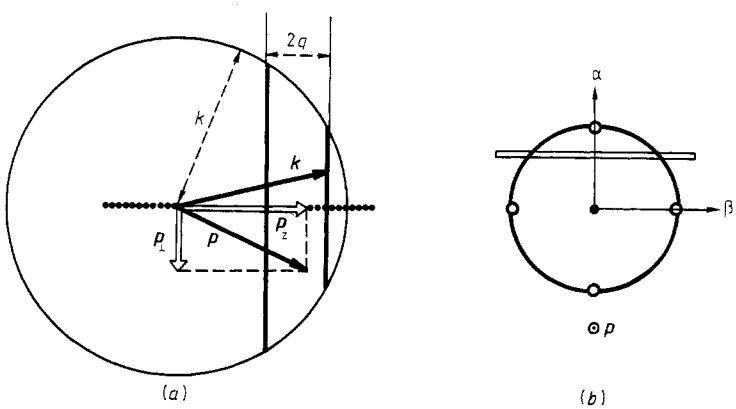

Figure 3. (*a*) shows the geometry (not to scale) that the vectors $\boldsymbol{p}$, $\boldsymbol{k}$ and $\boldsymbol{q}$ must satisfy in the one-dimensional situation. The molecular chain is represented by the horizontal dotted line. The head of vector $\boldsymbol{k}$ may lie along two circles (bold parts of the two vertical lines) which are the intersections of a sphere of radius k and two parallel planes separated by a distance $2q$. The direction of $\boldsymbol{k}$ is determined by two angles α and β as in figure 2.
(*b*) shows one of these circles represented in the (α, β) space. The black dot at the centre represents the chain axis, the circled dot ⊙ represents vector $\boldsymbol{p}$. The appropriate orientation of the detector slit to locate α_M (top open circle) is also shown.

sample. The intersection being obviously circles, its expression in the (α, β) space will be given by

$$k^2 = k_0^2 + P(\alpha^2 + \beta^2) \tag{25}$$

an expression which has to be equivalent to (10) with q given by (24) or equivalently by

$$q^2 = (p_z - k)^2 + k(p_z - k)(\alpha^2 + \beta^2)$$

(α and β are assumed to be small). Momentum k_0 in (25), and associated q_0, are obtained by solving (10) and (24) for $\alpha = \beta = 0$. These two equations are

$$p^2 - k_0^2 - \nu(q_0) = 0 \tag{26a}$$

$$q_0 = |p_z - k_0|. \tag{26b}$$

Then proceeding to the expansion of (10) for small $k^2 - k_0^2$, with q_0 defined by (24), one finds an expression for P which is the same as (15*a*) (with p_z replacing $p_\parallel$). A glance at (25) shows that the intersection (circle) exists as long as P and $k - k_0$ have the same sign. This means that both k and p_z have to be smaller or larger than k_0.

By using (25) and related expansions, the differential cross section (9) takes a form similar to (17). One has

$$\sigma(k, \alpha, \beta)/L = [S/(D(\alpha, \beta))^2]\delta(k^2 - k_0^2 - P(\alpha^2 + \beta^2)) \tag{27}$$

with $D(\alpha, \beta)$ defined as in (19) but with S given by

$$S = m^2 e^2 \nu(q_0)/[p^4 \ln(a/q_0)]. \tag{28}$$

Experimentally, one should determine the extremal angles α_M and β_M which are equal, and are represented by open circles in figure 3(*b*). Angle α_M is probably easier to measure than β_M. The beam is scanned by a slit placed parallel to the sample surface

where the one-dimensional chains are surfacing. The scanning is along the α axis and one measures

$$L^{-1}\sigma(k,\alpha) = L^{-1}\int_{-\Delta\beta}^{\Delta\beta} \mathrm{d}\beta\, \sigma(k,\alpha,\beta)$$
$$= S\Theta(\mathcal{B})/[D(\alpha,\sqrt{\mathcal{B}})^2|P|\sqrt{\mathcal{B}}]. \tag{29}$$

with $\mathcal{B} = (k^2 - k_0^2)/P - \alpha^2$. As before this cross section has a sharp peak for $\mathcal{B} = 0$ followed by a cancellation. This structure appears for α_M given by the same expression as (23). Here again the detection of α_M as a function of k^2 will give direct information on the parameters defining the plasmon dispersion relation. In the next section we will make a numerical application of this theory assuming an accepted form for the plasmon dispersion relation. As input data we will use the parameters already suggested in literature for the quasi-one-dimensional conductors. These parameters indicate that α_M should be detectable in this case.

4. Applications to specific physical systems

Let us write the plasmon dispersion relation in the general form

$$\nu(q) = \nu(0) + \mu q^n \tag{30}$$

as mentioned in the Introduction. Besides the zero momentum plasmon energy $\nu(0)$, the main parameters of (30) are μ and n. Our aim is to determine these parameters experimentally by ricochet scattering. The differential cross section is given by (20) or by (22). The experimental technique consists in collecting the scattered electrons for a well defined outgoing energy $k^2/2m$ and then detecting the peak by a slit detector in the cross section either along the β or the α direction. This peak appears at $\beta = \beta_M(k^2)$ given by (21), or at $\alpha = \alpha_M(k^2)$ given by (23). The important point to realise is that β_M^2, or α_M^2, is proportional to $k^2 - k_0^2$ and basic information can be obtained from the slope

$$\Delta\beta_M^2/\Delta k^2 = 2q_0/p^2\nu'(q_0) = 2q^{2-n}/n\mu p^2 \tag{31a}$$

or

$$\Delta\alpha_M^2/\Delta k^2 = \pm 2/p\nu'(q_0) = \pm 2q^{1-n}/n\mu p \tag{31b}$$

which can be obtained from the experimental determination of α^2 or β^2. Other information comes from the limit $\beta^2 \to 0$ in (21), or $\alpha^2 \to 0$ in (23), which, when obtained by linear extrapolation of the experimental data, yields

$$k_0^2 = \lim k^2. \tag{32}$$

Parameters n and μ are thus obtained from these data, and from these expressions (31) and (32) where approximate values of q_0 and k_0 can be introduced, namely

$$\tilde{q}_0 = |p_\parallel - (p^2 - \nu(0))^{1/2}| \tag{33}$$

and

$$\tilde{k}_0 = (p^2 - \nu(q_0))^{1/2} \tag{34}$$

which are the solutions of (14) after a first-order iteration. Note that for 'acoustic' plasmons, where $\nu(0) = 0$, (33) has a simpler form

$$\tilde{q}_0 = p - p_\parallel \simeq p\theta^2/2 \tag{35}$$

showing that q_0 is very sensitive to the choice of the incidence angle θ.

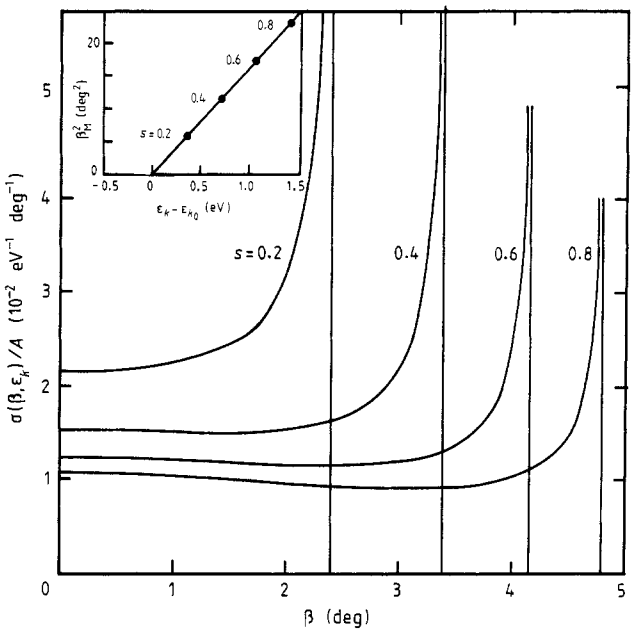

Figure 4. Scattering cross section $\sigma(\beta, \varepsilon_k)$ plotted as a function of β for four values of outgoing energy ε_k. Here surface plasmons are excited on an aluminium sample. The incident electron energy is 100 eV with $\theta = 2°$, and the outgoing energy is $\varepsilon_k = [88.84 - 1.75(1 - s)]$ eV. The vertical lines correspond to the critical angle $\beta_M = 5.36°\sqrt{s}$. The inset shows a plot of β_M^2 against $\varepsilon_k - \varepsilon_{k_0}$, with s values indicated by dots. Note that the slope of this line gives information on μ.

4.1. Surface plasmon on a metal sample

As a first application we consider the excitation of a surface plasmon on the surface of an aluminum sample. We will present a numerical result by assuming a linear dispersion rule ($n = 1$) calculated in the hydrodynamical model (Ritchie 1963, Ritchie and Marusak 1966).

In this model, the general form (30) becomes $\nu(q) = 2m\omega_s + \mu q$ with $\omega_s = \omega_p/\sqrt{2} = 11.16$ eV (ω_s and ω_p being the surface and bulk plasmon frequencies, respectively) and $\mu = (3/5)^{1/2}k_F$, i.e. $\mu^2/2m = 3\varepsilon_F/5 = 6.99$ eV. Using these numbers and an incident beam with an energy $\varepsilon_p = p^2/2m = 100$ eV and an incidence angle $\theta = 2°$, we obtain the cross section $\sigma(\varepsilon_k, \beta)$ from (20) as represented in figure 4. Here we have written the outgoing energies in the form

$$\varepsilon_k = \varepsilon_{edge} - (1 - s)\mu q_0/2m$$

with $\varepsilon_{edge} = \varepsilon_p - \omega_s = 88.84$ eV, or equivalently

$$\varepsilon_k = \varepsilon_{k_0} + s\mu q_0/2m \tag{36}$$

where q_0 and k_0 are obtained by solving (14). One has $q_0^2/2m = 0.44$ eV and $\varepsilon_{k_0} = k_0^2/2m = 87.09$ eV. This latter quantity being smaller than $p_\parallel^2/2m = 99.88$ eV, we are in the situation depicted by figure 2(b). The four curves of figure 4 correspond to $s = 0.2$, 0.4, 0.6 and 0.8. The related outgoing energies thus differ by a quantity

$0.2\,\mu q_0/2m = 0.35$ eV which should be detectable experimentally. From (21) and (36), one obtains

$$\beta_M^2 = 2q_0^2 s/p^2$$

giving the critical angle where the curves of figure 4 are peaking. Using our numbers we have $\beta_M = 5.36°\sqrt{s}$ and from (31*a*) with $n = 1$, we obtain

$$\Delta\beta_M^2/\Delta\varepsilon_k = 4mq_0/\mu p^2 = 16.43 \text{ deg}^2 \text{ eV}^{-1}$$

a slope which appears in the inset of figure 4 and which should be compared with experimental data. Such a comparison will give a check of the linearity of the dispersion relation ($n = 1$), as well as of the appropriateness of the μ value. A determination of ε_{k_0}, and hence ω_s, can also be obtained for $\beta_M \to 0$ as shown in this inset.

In the problem of the surface plasmons of metals, the β scanning is probably much more sensible than the α scanning which the authors had suggested in their previous paper (Longe and Bose 1986). However, for the next applications (acoustic plasmons), the α scanning will definitely be preferable.

4.2. Two-dimensional plasmon in the accumulation layers on ZnO

As a second application of ricochet scattering of electrons by a two-dimensional plasmon, we now consider the accumulation layers (Goldstein *et al* 1980, Many *et al* 1981). These are two-dimensional electron gases (2DEG) directly accessible to electron scattering experiments. Unlike the usual MOS structure (Stern 1967, Ando *et al* 1982, Fetter 1973, Vinter 1975, Allen *et al* 1977, Giuliani and Quinn 1984), they are not covered by an oxide layer. The accumulation layers on ZnO are found to be particularly strong (Goldstein *et al* 1980, Many *et al* 1981).

In the appendix, we have mentioned that the plasmon dispersion relation is given by the cancellation of $1 + v_0 B_R$ in the denominator of propagator (A5) and that B_R is proportional to ω^{-2} for small q. More precisely in the RPA one has $B_R = -n_D q^2/m\omega^2$, an expression valid for an electron gas of dimension D which can be established from (A7) (n_D is the electron density). Since for a 2DEG one has $v_0(q) = 2\pi e^2/q$ (see § 2) one finds

$$\omega_2(q) = (2\pi e^2 n_2 q/m)^{1/2}. \tag{37}$$

This well known result shows that for a 2DEG one should expect acoustic plasmons with a dispersion relation of the form

$$\nu(q) = \mu q^{1/2}. \tag{38}$$

Using the above relation with $n_2 = 2 \times 10^{13}\,\text{cm}^{-2}$, a density currently met in ZnO accumulation layers, we can write $\mu = 0.119\,a_B^{-3/2}$ where a_B is the Bohr radius. An appropriate choice for the incident beam is an energy $\varepsilon_p = 400$ eV and an incidence angle $\theta = 4°$. Introducing these numbers in (14) one finds $q_0 = 0.0120\,a_B^{-1}$ (or $q^2/2m = 1.96$ meV), $v(q_0) = 0.0130\,a_B^{-2}$ (or $\omega_2(q_0) = 0.177$ eV) and $\varepsilon_{k_0} = (400 - 0.177)$ eV. Energy ε_{k_0} is thus larger than $p_\parallel^2/2m = 398$ eV and we have the situation depicted by

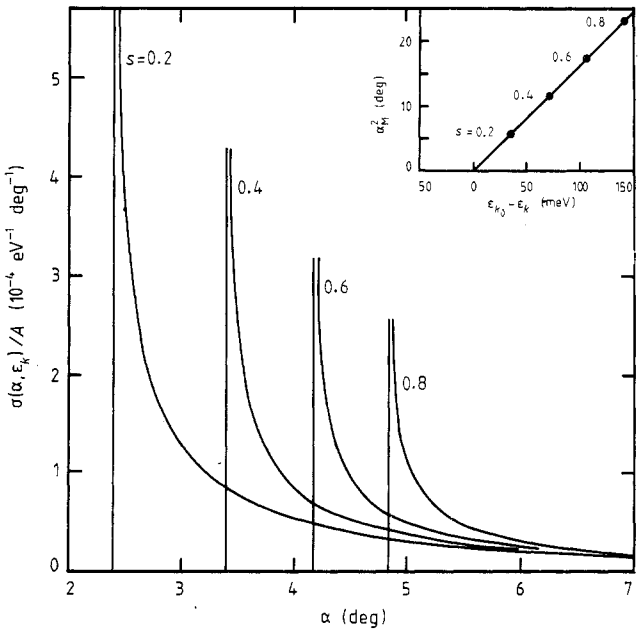

Figure 5. Scattering cross section $\sigma(\alpha, \varepsilon_k)$ plotted as a function of α for four values of outgoing energy ε_k. Here two-dimensional plasmons are excited in a 2DEG (accumulation layer on ZnO). The incident electron energy is 400 eV with $\theta = 4°$, and the outgoing energy is $\varepsilon_k = [400 - 0.177(1 + s)]$ eV. The vertical lines correspond to the critical angle $\alpha_M = 5.39°\sqrt{s}$. The inset plots α_M^2 against $\varepsilon_{k_0} - \varepsilon_k$, with s values indicated by dots. Here again the slope of this line gives direct information on μ.

figure 2(*c*). The related differential cross section $\sigma(\varepsilon_k, \alpha)$ computed from (22) is represented in figure 5 where we write the outgoing energies in the form

$$\begin{aligned}\varepsilon_k &= \varepsilon_p - (1 + s)\omega_2(q_0) \\ &= \varepsilon_{k_0} - s\omega_2(q_0).\end{aligned} \tag{39}$$

The four curves of figure 5 correspond to $s = 0.2, 0.4, 0.6$ and 0.8. The outgoing energies considered differ by a quantity $0.2\,\omega_2(q_0) = 35.4$ meV which is small but should be detectable. The peaks occur for critical angles given by

$$\alpha_M^2 = (4q_0/p)s$$

as shown by (23) and (39). More explicitly one has $\alpha_M = 5.39° \sqrt{s}$. The inset of figure 6 depicts the slope

$$\Delta\alpha_M^2/\Delta\varepsilon_k = -8m(\sqrt{q_0})/\mu p = -164.2\ \text{deg}^2\ \text{eV}^{-1}$$

given by (31*b*) with $n = \frac{1}{2}$, from which the validity of (38) and the choice of μ can be checked. Note that the validity of (38), or in other words the value of $n = \frac{1}{2}$ of the exponent can be verified easily by considering the dependence of that slope on q_0 as given by (31*b*). For acoustic plasmons q_0 is indeed proportional to the square of incidence angle θ as shown in (35) and its value can thus be easily modified and controlled.

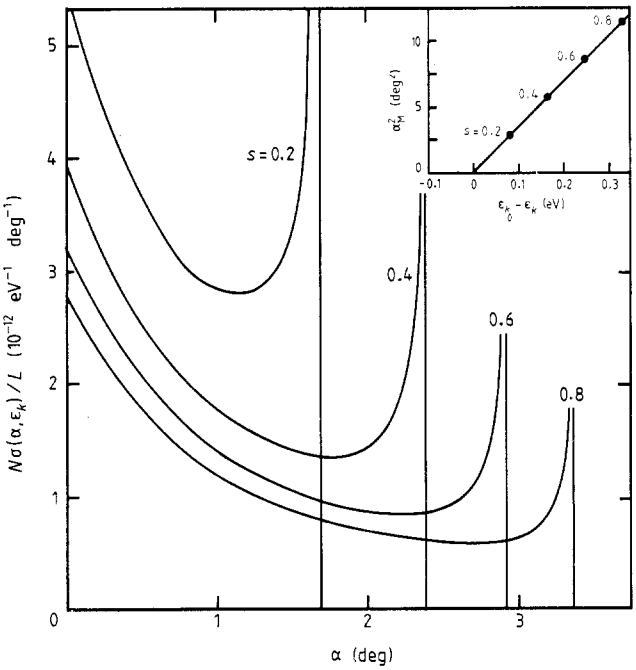

Figure 6. Scattering cross section $\sigma(\alpha, \varepsilon_k)$ plotted as a function of α for four values of outgoing energy ε_k. Here plasmons are excited in a one-dimensional conductor of length L (if one considers a set of parallel conductors displayed on a surface, N is their density per transverse unit length). The incident electron energy is 400 eV with $\theta = 4°$, and the outgoing energy is $\varepsilon_k = [40 - 0.419(1 + s)]$ eV. The vertical lines correspond to the critical angle $\alpha_M = 3.77°\sqrt{s}$.

4.3. One-dimensional conductors

In this last application the one-dimensional plasmon (Williams and Bloch 1974, Apostol 1975, Campos *et al* 1977, Friesen and Bergersen 1980, Kaner and Chebotarev 1985, Das 1986) is often described by a logarithmic dispersion relation, which is somewhat more complicated than (30). However, the ricochet scattering may still be used to obtain its parameters. For the present discussion an appropriate model dispersion relation should be introduced. Again we refer back to propagator (A5) in the appendix, where this relation is obtained from the cancellation of the denominator, i.e. by setting $1 + v_0 B_R = 0$. Again we use the RPA expression $B_R = -n_D q^2/m\omega^2$ and the potential $v_0 = 2e^2 \ln(a/q)$ already presented in § 2. This gives the dispersion relation

$$\omega_1(q) = q[2e^2 n_1 \ln(a/q)/m]^{1/2}. \tag{40}$$

Such a relation has been discussed by many authors. Let us write it in the form

$$\nu(q) = \mu q(\ln a/q)^{1/2} \tag{41}$$

where in the RPA we have $\mu^2 = 8n_1/a_B$. The aim of ricochet scattering is to determine μ and a in (41). To present a numerical example, let us write† $\mu = 1.427\, a_B^{-1}$ and

† Referring for instance to the parameters K, U and A introduced by Friesen and Bergersen (1980), these numbers correspond to the choice $K = 1$, $U = 5$ and $A = 0.5$. These authors define their parameters as $U = 2/a_B k_F = 4/\pi a_B n$, and $A = k_\Gamma/a$; K is a dielectric constant.

$a = 0.8\,a_B^{-1}$ and assume an incident beam with an energy $\varepsilon_p = 400$ eV and an incidence angle $\theta = 4°$. Introducing these values in (14) one finds $q_0 = 0.0104\,a_B^{-1}$ (or $q^2/2m = 1.46$ meV), $\nu(q_0) = 0.0308\,a_B^{-2}$ (or $\omega_1(q_0) = 0.419$ eV) and $\varepsilon_{k_0} = (400 - 0.419)$ eV. The differential cross section given by (29) can then be computed and is represented in figure 6 where the outgoing energies are written in the form

$$\varepsilon_k = \varepsilon_p - (1 + s)\omega_1(q_0) = \varepsilon_{k_0} - s\omega_1(q_0). \tag{42}$$

The four curves of figure 6 correspond to $s = 0.2, 0.4, 0.6$ and 0.8. The outgoing energies considered thus differ by $0.2\ \omega_1(q_0) = 83.9$ meV which should also be detectable. The peaks occur for critical angles given by

$$\alpha_M^2 = 2q_0/pL(a/q_0)s \tag{43}$$

with $L(x) = \ln x/(\ln x - \frac{1}{2})$, as shown by (23) and (42). More explicitly one has $\alpha_M = 3.77° \sqrt{s}$. The inset of figure 6 gives the slope

$$\Delta\alpha_M^2/\Delta\varepsilon_k = -(4m/\mu p)(\ln(a/q_0))^{-1/2}L(a/q_0) = -33.8\ \text{deg}^2\ \text{eV}^{-1}$$

obtained from (42) and (43). This slope should be determined experimentally to yield information on the dispersion rule. Note that as long as $a \gg q_0$, which is the case in the present numerical study, one has $L(a/q_0) \simeq 1$ (here $(L(a/q_0) = 1.13)$ and the slope $\Delta\alpha_M^2/\Delta\varepsilon_k$ depends only weakly on q_0. This is probably the most interesting feature which could be checked by ricochet scattering in this one-dimensional situation. Indeed it seems rather difficult to discriminate between the roles played independently by μ and a in a dispersion relation like (41). However, if ricochet scattering measurements yield a slope $\Delta\alpha_M^2/\Delta\varepsilon_k$ which appears to be too sensitive to q_0 (q_0 is proportional to θ^2 as shown by (35)), this means that the expression (41) for the dispersion relation has to be reconsidered.

Acknowledgment

One of the authors (PL) is grateful to the Fonds National de la Recherche Scientifique, Belgium, for financial support.

Appendix

In this appendix we present the calculation of $U(\boldsymbol{q}, \boldsymbol{x}_\perp)$ which appears in the expression for the scattering cross section given in (6).

To calculate $U(\boldsymbol{q}, \boldsymbol{x}_\perp)$ we note that this potential appears in (6) as a factor

$$\pi\delta(\omega - \omega_D(q))U(\boldsymbol{q}, \boldsymbol{x}_{2\perp})U(\boldsymbol{q}, \boldsymbol{x}_{1\perp}) \tag{A1}$$

which is the imaginary part of the effective potential between two charges located at $\boldsymbol{x}_1$ and $\boldsymbol{x}_2$ *outside* the electron gas, but interacting *via* the electron gas. In the position space, this potential is given by

$$\int \mathrm{d}^D x'_{2\|} \int \mathrm{d}^D x'_{1\|} v(\boldsymbol{x}_{2\|} - \boldsymbol{x}'_{2\|}, \boldsymbol{x}_{2\perp})F(\boldsymbol{x}'_{2\|} - \boldsymbol{x}'_{1\|}, \omega)v(\boldsymbol{x}'_{1\|} - \boldsymbol{x}_{1\|}, \boldsymbol{x}_{1\perp})$$

where $v(\boldsymbol{x}_\|, \boldsymbol{x}_\perp) = v(\boldsymbol{x}) = e^2/|\boldsymbol{x}|$ is the Coulomb potential and $F(\boldsymbol{x}'_{2\|} - \boldsymbol{x}'_{1\|}, \omega)$ is the density

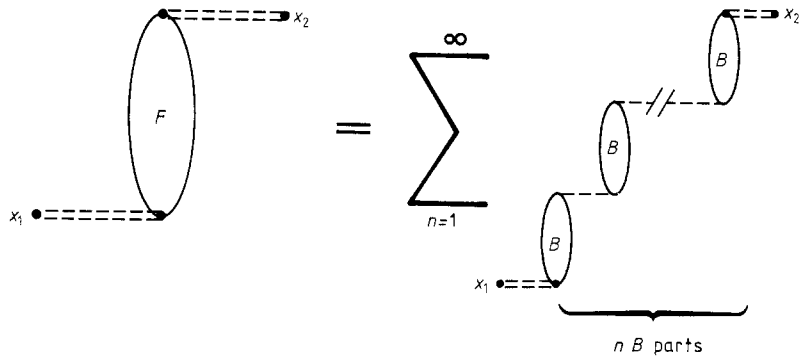

Figure 7. Diagram representing the effective potential between two charges located at $\boldsymbol{x}_1$ and $\boldsymbol{x}_2$ *outside* the electron gas but interacting *via* the electron gas.

fluctuation propagator inside the electron gas (hence $\boldsymbol{x}'_{1\perp} = \boldsymbol{x}'_{2\perp} = 0$). The Fourier transform of this effective potential (related to the internal coordinates of the electron gas) is given by

$$v(\boldsymbol{q}, \boldsymbol{x}_{2\perp})F(\boldsymbol{q}, \omega)v(\boldsymbol{q}, \boldsymbol{x}_{1\perp}) \tag{A2}$$

which is an expression represented by the left-hand side member of the diagrammatic equation of figure 7. Since we only consider that part of propagator F which concerns the collective plasmon excitation, F has the form

$$F(\boldsymbol{q}, \omega) = -C(\boldsymbol{q})/(\omega - \omega_{\mathrm{D}}(q) + \mathrm{i}\lambda) \tag{A3}$$

and looking at (A1) and (A2), we can thus write

$$U(\boldsymbol{q}, \boldsymbol{x}_\perp) = v(\boldsymbol{q}, \boldsymbol{x}_\perp)(C(\boldsymbol{q}))^{1/2}. \tag{A4}$$

Now the problem consists in determining the amplitude factor $C(\boldsymbol{q})$ in (A3). Let us write $F(\boldsymbol{q}, \omega)$ as

$$F(\boldsymbol{q}, \omega) = B(\boldsymbol{q}, \omega)/(1 + v_0(\boldsymbol{q})B(\boldsymbol{q}, \omega)) \tag{A5}$$

where $B(\boldsymbol{q}, \omega)$ is the irreducible polarisation part of $F(\boldsymbol{q}, \omega)$ in the D-dimensional electron gas, the electron–electron potential being $v_0(\boldsymbol{q}) = v(\boldsymbol{q}, \boldsymbol{x}_\perp)$ with $\boldsymbol{x}_\perp = 0$. In the diagrams of figure 7, the difference between $v_0(\boldsymbol{q})$ appearing in (A5) and $v(\boldsymbol{q}, \boldsymbol{x}_\perp)$ appearing in (A2) is shown by using a single broken line for v_0 and a double one for v. The plasmon energy $\omega = \omega_{\mathrm{D}}(q)$ comes out from (A5) as a solution of $1 + v_0(\boldsymbol{q})B_{\mathrm{R}}(\boldsymbol{q}, \omega) = 0$ for a vanishing $B_{\mathrm{I}}(\boldsymbol{q}, \omega)$ (B_{R} and B_{I} are the real and the imaginary part of B, respectively.). Expanding the denominator of (A5) about $\omega \sim \omega_{\mathrm{D}}$ one finds (A3) with

$$C(\boldsymbol{q}) = -[B_{\mathrm{R}}(\boldsymbol{q}, \omega)/(v_0(\boldsymbol{q})\partial B_{\mathrm{R}}(\boldsymbol{q}, \omega)/\partial\omega)]_{\omega=\omega_{\mathrm{D}}}. \tag{A6}$$

This expression of the amplitude factor $C(\boldsymbol{q})$ is quite general. For a more explicit calculation we can use the RPA where the polarisation part for a D-dimensional electron gas is

$$B(\boldsymbol{q}, \omega) = \frac{2\mathrm{i}}{(2\pi)^{D+1}} \int \mathrm{d}^D k \int \mathrm{d}\omega' \left(\frac{\Theta(k_{\mathrm{F}} - k)}{(\omega' - \varepsilon_k - \mathrm{i}\lambda)} \frac{\Theta(|\boldsymbol{k}+\boldsymbol{q}| - k_{\mathrm{F}})}{(\omega + \omega' - \varepsilon_{|\boldsymbol{k}+\boldsymbol{q}|} + \mathrm{i}\lambda)} + \mathrm{i}d(\omega \rightarrow -\omega) \right) \tag{A7}$$

k_F being the radius of a Fermi D-sphere. For small values of q it can be shown that the real part of this expression is proportional to ω^{-2} yielding $B_R[\partial B_R/\partial\omega]^{-1} = -\omega/2$. Hence from (A6) and (A4) one has

$$U(\boldsymbol{q}, \boldsymbol{x}_\perp) = v(\boldsymbol{q}, \boldsymbol{x}_\perp)(\omega_D(q)/2v_0(\boldsymbol{q}))^{1/2} \tag{A8}$$

which can be introduced into the expression (6) of the differential cross section.

References

Allen S J Jr, Tsui D C and Logan R A 1977 *Phys. Rev. Lett.* **38** 980–3
Ando T, Fowler A B and Stern F 1982 *Rev. Mod. Phys.* **54** 437–672
Apostol M 1975 *Z. Phys.* B **22** 279–83
Bose S M, Kiehm P and Longe P 1981 *Phys. Rev.* B **23** 712–23
Bose S M, Prutzer S and Longe P 1983 *Phys. Rev.* B **27** 5992–9
Campos V B, Hipolito O and Lobo R 1977 *Phys. Stat. Sol.* b **81** 657–63
Das A K 1986 *J. Phys. F: Met. Phys.* **16** L99–L102
Fetter A L 1973 *Ann. Phys., NY* **81** 367–93
Friesen W I and Bergersen B 1980 *J. Phys. C: Solid State Phys.* **13** 6627–40
Giuliani G F and Quinn J J 1984 *Phys. Rev.* B **29** 2321–3
Goldstein Y, Many A, Wagner I and Gersten J 1980 *Surf. Sci.* **98** 599–612
Grimes C C 1978 *Surf. Sci.* **73** 379–95
Kaner E A and Chebotarev L V 1985 *J. Stat. Phys.* **38** 77–87
Longe P and Bose S M 1986 *Phys. Rev. Lett.* **57** 2307–10
Many A, Wagner I, Rosenthal A, Gersten J I and Goldstein Y 1981 *Phys. Rev. Lett.* **46** 1648–51
Ritchie R H 1963 *Prog. Theor. Phys.* **29** 607–8
Ritchie R H and Marusak A L 1966 *Surf. Sci.* **4** 234–40
Stern F 1967 *Phys. Rev. Lett.* **18** 546–8
Vinter B 1975 *Phys. Rev. Lett.* **35** 1044–7
Williams P F and Bloch A N 1974 *Phys. Rev.* B **10** 1097–108